Article

Discovery Medicine 2023; 35(177): 612–622
https://doi.org/10.24976/Discov.Med.202335177.60

FMO1 Promotes Nonalcoholic Fatty Liver Disease Progression by Regulating PPARα Activation and Inducing Ferroptosis

Lin Zou[1,†], Qin Shi[2,†], Yingxuan Li[1], Zhen Yuan[1], Li Peng[1], Jiancan Lu[1], Hongling Zhu[1,*], Junhua Ma[1,*]

[1]Department of Endocrinology, Gongli Hospital of Shanghai Pudong New Area, 200135 Shanghai, China
[2]Department of General Practice, Gongli Hospital of Shanghai Pudong New Area, 200135 Shanghai, China
*Correspondence: zhl_med@163.com (Hongling Zhu); jhmagl@126.com (Junhua Ma)
†These authors contributed equally.
Published: 1 August 2023

Background: The function of flavin containing dimethylaniline monooxygenase 1 (FMO1), which is known to play a part in lipid metabolism, remains unclear in the development of nonalcoholic fatty liver disease (NAFLD). This research has the objective of examining the contributions of FMO1 in the progression of NAFLD and the associated mechanisms, particularly the peroxisome proliferator activated receptor alpha (PPARα) and ferroptosis pathways.

Methods: An *in vitro* NAFLD model was established by treating L02 cells with free fatty acids (FFAs). The FMO1 and ferroptosis levels were examined in the cellular NAFLD model. *FMO1* was knocked down using short-interfering RNA transfection. The effects of *FMO1* knockdown on lipid accumulation, PPARα expression, and ferroptosis were examined in the cellular NAFLD model. Additionally, the effects of *FMO1* and/or *PPARα* overexpression on lipid metabolism and ferroptosis were analyzed. Furthermore, L02 cells were pre-treated with GW7647 (PPARα agonist) or RSL3 (ferroptosis activator) and stimulated with FFAs.

Results: The levels of FMO1 and ferroptosis were upregulated in the *in vitro* NAFLD model. *FMO1* knockdown suppressed the FFA-induced accumulation of lipids in hepatocytes, downregulation of PPARα expression, and upregulation of ferroptosis. In contrast, *FMO1* overexpression dysregulated lipid metabolism and downregulated PPARα levels. Meanwhile, *PPARα* overexpression mitigated the *FMO1* overexpression-induced upregulation of ferroptosis and lipid accumulation. Treatment with RSL3 suppressed the effects of *PPARα* overexpression on lipid accumulation and FMO1 expression.

Conclusions: FMO1 upregulates ferroptosis by suppressing PPARα in NAFLD, which leads to the dysregulation of lipid metabolism.

Keywords: nonalcoholic fatty liver disease; FMO1; PPARα; ferroptosis; lipid metabolism

Introduction

Nonalcoholic fatty liver disease (NAFLD) is a liver disease caused by metabolic stress, characterized by abnormal buildup of lipids in liver cells [1]. The progression of NAFLD is linked to liver inflammation and an increased risk of liver cirrhosis, failure, and cancer [2,3]. In the United States and Europe, the prevalence rates of NAFLD range from 25% to 30% [4], while in China, it is 27% [5]. Despite its high prevalence, the causes and mechanisms of NAFLD remain unclear [6]. As a result, understanding the mechanisms behind NAFLD and identifying new therapeutic targets have become important areas of research in hepatology.

Ferroptosis, an innovative process of cellular demise, occurs due to the abnormal peroxidation of unsaturated fatty acids on the cell membrane, which is mediated by ferrous ions [7]. Glutathione peroxidase 4 (GPX4), a selenoprotein, efficiently reduces peroxidized phospholipids. The inactivation of glutathione (GSH) induced by GPX4 depletion promotes ferroptosis [8,9]. The activation of ferroptosis affects hepatocyte function and induces inflammation [10]. The liver is involved in lipid metabolism and stores iron. Lipid peroxides directly induce ferroptosis, which subsequently promotes the progression of NAFLD to inflammation and fibrosis [11,12]. The mechanisms involved in regulating ferroptosis in NAFLD have not been elucidated.

Peroxisome proliferator activated receptor alpha (PPARα) is a ligand-dependent transcriptional regulator with a critical role in glycolipid metabolism and inflammatory responses [13]. A recent clinical study reported that pemafibrate, a PPARα modulator, can suppress NAFLD progression and NAFLD-related inflammation and fibrosis [14]. Furthermore, PPARα is reported to regulate fer-

roptosis [15]. PPARα can alleviate hepatocyte ferroptosis by promoting *GPX4* transcription [16]. However, the regulatory effects of PPARα on ferroptosis in NAFLD are unclear. Previous studies have demonstrated that flavin containing dimethylaniline monooxygenase 1 (FMO1) is significantly upregulated in NAFLD [17]. Although FMO1 is reported to be involved in lipid metabolism, its correlation with lipid accumulation in NAFLD is unclear [18]. FMO1 can regulate PPARα and mediate metabolic processes [19]. However, the effects of FMO1 on lipid metabolism and ferroptosis in NAFLD and the role of PPARα have not been examined.

In this study, the regulatory effects of FMO1 on NAFLD through PPARα, as well as on ferroptosis and lipid accumulation, were examined. This study aimed to complement the current understanding of the role of ferroptosis in NAFLD and provide useful insights for the treatment of NAFLD.

Materials and Methods

Cells Culture

The L02 cells, which are healthy human hepatocytes (Shanghai Academy of Sciences, Shanghai, China), were cultured in Dulbecco's modified Eagle medium (DMEM)/F12 medium (Gibco, Carlsbad, CA, USA) supplemented with 10% fetal bovine serum (Gibco, Carlsbad, CA, USA), penicillin (100 U/mL) and streptomycin (100 µg/mL) under 37 °C in a 5% CO_2 incubator. The cultured cells were analyzed for mycoplasma infection, and the results indicated no presence of infection. Additionally, the L02 cells underwent short tandem repeat analysis. The specific methods and cell grouping are described below.

Experiment 1: FMO1 Knockdown and Free Fatty Acid (FFA) Intervention

The cells were categorized into the following groups: the Control; the FFA group, cells were treated with FFA (oleate:palmitate = 2:1, 0.5 mmol/L) for 24 hours to develop the NAFLD model *in vitro*; the group known as short-interfering RNA (siRNA) against FMO1 (si-FMO1) consisted of cells that were transfected with si-FMO1; the FFA + si-FMO1 group, consisted of cells that were incubated with FFA and transfected with si-FMO1.

Experiment 2: Overexpression of FMO1 and PPARα

The cells were assigned into Control (transfected with empty vector); FMO1 group (cells were treated with *FMO1*-overexpression plasmid); PPARα group (cells were treated with *PPARα*-overexpression plasmid); FMO1 + PPARα group (cells were treated with *FMO1*-overexpression and *PPARα*-overexpression plasmids).

Experiment 3: Ferroptosis and FFA-Induced NAFLD

The cells were categorized into several groups: Control group was composed of untreated cells; FFA group consisted of cells treated with FFA (oleate:palmitate = 2:1, 0.5 mmol/L) for 24 hours to create the *in vitro* NAFLD model. The FFA + GW7647 group involved cells pre-treated with 10 µM GW7647 (PPARα agonist) for 24 hours and then treated with 0.5 mmol/L FFA mixture for 24 hours. In the FFA + RSL3 group, cells were pre-treated with RSL3 (ferroptosis activator, 5 µmol/L) for 24 hours and then treated with 0.5 mmol/L FFA mixture for 24 hours. Finally, in the FFA + GW7647 + RSL3 group, cells were pre-treated with both 10 µM GW7647, 5 µmol/L RSL3 and 0.5 mmol/L FFA mixture for 24 hours.

Cell Treatment

Cells cultured in DMEM/F12 medium (Gibco, Carlsbad, CA, USA) were incubated at 37 °C and 5% CO_2 in an incubator until they reached 80% confluence and starved in serum-free medium overnight prior to treatment. In order to establish the *in vitro* NAFLD model, the cells were treated with an FFA mixture (oleate:palmitate = 2:1) at a final concentration of 0.5 mmol/L in the culture medium for 24 h [20].

To activate PPARα, the cells were pre-treated with 10 µM GW7647 (Sigma-Aldrich, St. Louis, MO, USA) for 24 h, and then stimulated with FFA for 24 h. The negative control consisted of cells pre-treated with vehicle (dimethyl sulfoxide (DMSO)) for 24 h and then treated with FFA for 24 h [21]. To induce ferroptosis, the cells were pre-treated with 5 µmol/L RSL3 (Selleck Chemical, Houston, TX, USA) for 24 h, followed by treatment with FFA for 24 h. The negative control consisted of cells pre-treated with vehicle (DMSO) for 24 h and then treated with FFA for 24 h [22].

Cell Transfection

L02 cells were treated with *si-FMO1*, *FMO1* overexpression, or *PPARα* overexpression plasmids (GenePharma Co., Ltd., Shanghai, China) using lentiviral vectors. Cells transfected with negative control (NC) vector or si-NC served as controls. For *si-FMO1* transfection, cells were seeded in a 6-well plate (5×10^4 cells/well) and transfected with *si-FMO1* for 24 h, then treated with FFA for 24 h. These siRNA sequences were used in the study: *si-FMO1*, 5′-CACUGGCUUUCUUACUAAUCCUUAU-3′ (sense sequence) and 5′-AUAAGGAUUAGUAAGAAAGCCAGUG-3′ (antisense sequence); si-NC, 5′-CACUUCGUUCUAUCACCUAUGUUAU-3′ (sense sequence) and 5′-AUAACAUAGGUGAUAGAACGAAGUG-3′ (antisense sequence).

To achieve overexpression of *FMO1* or *PPARα*, L02 cells were initially plated in a 6-well plate at a density of 5×10^4 cells per well. Subsequently, 50 pmol (0.67 µg) of overexpression plasmids for *FMO1* or *PPARα* were diluted in 25 µL serum-free DMEM, referred to as reagent A. Reagent

B was created by incubating 1 µL of EntransterTM-R4000 (Engreen Biosystem Co., Ltd., Beijing, China) with 24 µL serum-free DMEM for a duration of 25 minutes. Both reagent A and reagent B, each composed of 25 µL, were thoroughly mixed by aspiration using a pipette for a total of 10 times. After allowing this mixture to remain undisturbed for 15 minutes.

Cell Viability

Various treatments were applied to L02 cells that were seeded in a 96-well plate (1×10^4 cells/well). Following the treatments, cells were exposed to cell counting kit-8 (CCK-8) solution from Beyotime, Shanghai, China, for 2 hours at 37 °C and with 5% CO_2 in an incubator. The optical density (OD) was measured to calculate the viability following the instruction.

Oil Red O Staining

After being fixed in 10% formalin for 15 minutes, L02 cells were treated with a washing solution for 20 minutes. Following the removal of the washing solution, the cells were treated with Oil Red O reagent (C0158M, Beyotime, Shanghai, China) for 20 minutes at 25 °C. Next, the cells were rinsed with phosphate-buffered saline for 20 seconds and counterstained with hematoxylin.

Triglyceride (TG) and Cholesterol Measurement

The enzymatic assay kit (E1025-105, E1026-105, Applygen Technologies Inc., Beijing, China) was applied to examine the levels of TGs and total cholesterol in cells. In a 96-well plate, 10 µL of the supernatant obtained after cells (2×10^6) were lysed in lysis buffer was mixed with the reactants for 30 min. Subsequently, the samples were treated with the developer for 15 min at 37 °C. A blank well was utilized for zero adjustment. The absorbance of the reaction mixture was measured at 450 nm to calculate the concentrations of TGs and total cholesterol.

Quantitative Real-Time Polymerase Chain Reaction (qRT-PCR)

The sample was homogenized through grinding, then incubated with 600 µL Trizol for 5 min, then centrifuged for 5 min (4 °C, 12,000 *g*). The supernatant was incubated with a mixture of Trizol and chloroform at a 1:2 ratio, and the samples were vigorously shaken for 15 s. Next, the aqueous phase was incubated with isopropanol to precipitate RNA. RNA was dissolved in diethyl pyrocarbonate-treated water, then reverse-transcribed into complementary DNA with a PrimeScript RT Reagent kit (RR047A, Takara, Tokyo, Japan). The conditions were 37 °C for 15 min; 98 °C for 5 min. qRT-PCR analysis was performed using SYBR Green reagent (Takara, Tokyo, Japan). The conditions were: 94 °C for 3 min, 40 cycles of 94 °C for 15 s, 58 °C for 20 s, and 72 °C for 30 s. The expression levels of *FMO1*, *PPARα*, and *GPX4* were determined using the $2^{-\Delta\Delta Ct}$ method after normalization with those of *GAPDH*. The following primers were used in qRT-PCR analysis: *FMO1*, 5′-TGGCACCAGAAATTACAAGTACG-3′ (forward) and 5′-AAAGCCAGTGCAGACCATGA-3′ (reverse); *PPARα*, 5′-CACACACCGAGGACTCTTGC-3′ (forward) and 5′-GCTCCAAGCTGTGGTGACA-3′ (reverse); *GPX4*, 5′-CCCATGTTGCGTTTTCCGAC-3′ (forward) and 5′-TCCAATGCATACAGGAAACTGGA-3′ (reverse); *GAPDH*, 5′-GTTTTCCGCCAAGGACATCG-3′ (forward) and 5′-ATAGTGGGGCAGGTCCTTCT-3′ (reverse).

Western Blotting

Cells were lysed and centrifuged at 4 °C and 12,000 *g* for 20 minutes. The protein samples were loaded onto a 12% gel and subjected to electrophoresis and transferred to a membrane. This membrane was then probed overnight at 4 °C with these primary antibodies: anti-FMO1 (1:800, PA5-95285, Thermo Fisher Scientific, Sunnyvale, CA, USA), anti-PPARα (1:1000, MA1-822, Thermo Fisher Scientific, Sunnyvale, CA, USA), and anti-GPX4 (1:800, ab252833, Abcam, Cambridge, MA, USA) and with a secondary antibody (1:2000, ab6721, Abcam, Cambridge, MA, USA) for 2 hours at 37 °C. To develop the immunoreactive signals, an enhanced chemiluminescence kit (Solarbio, Beijing, China) was used. The grayscale values of the protein bands were determined using IPP6.0 (Media Cybernetics Inc., Rockville, MD, USA).

Enzyme-Linked Immunosorbent Assay (ELISA)

The glutathione (GSH) concentration was detected using the GSH kit (S0052, Beyotime, Shanghai, China). The experimental settings were as follows: blank well (A), no sample or enzyme labeling reagent; standard well (B), 50 µL of the standard; sample well (C), 10 µL of the sample and 40 µL of diluent. The samples were thoroughly mixed and incubated with 50 µL of the enzyme labeling reagent at 37 °C for 30 min. Next, the samples were incubated with chromogenic reagents A and B (50 µL each) in the dark at 37 °C for 15 min. The OD at 450 nm of the reaction mixture was measured. The concentration of GSH in well C was calculated using the data of well A as the blank and those of well B as the standard. The GPX4 levels were examined using the GPX4 kit (EK-H12496, EK-Bioscience, Shanghai, China) with a similar ELISA procedure as described above.

Unstable Fe^{2+} Measurement

The detection of unstable Fe^{2+} levels was carried out using the FerroOrange probe (MX4559, MKbio, Shanghai, China). To ensure the powder settled at the bottom of the bottle, the thawed FerroOrange was centrifuged at low speed using a microcentrifuge. A stock solution of FerroOrange (1 mM) was added to 35 µL of DMSO in a tube containing 24 µg of FerroOrange. To ensure complete dissolution, the mixture was thoroughly mixed five times with

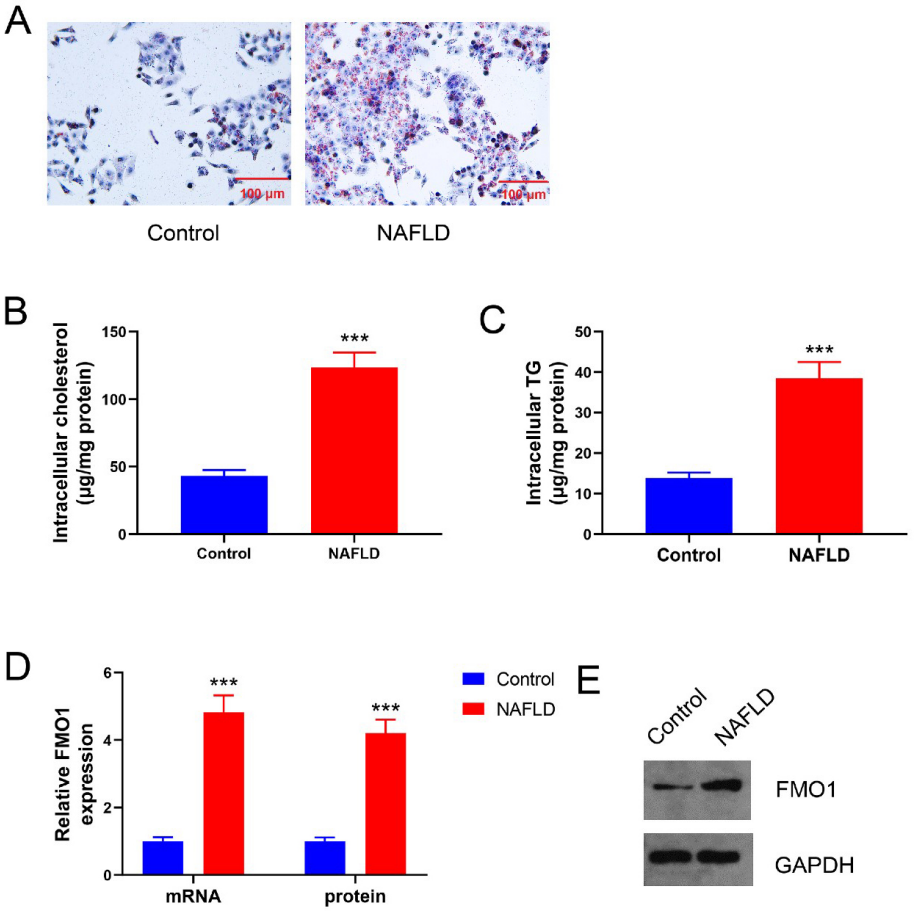

Fig. 1. Flavin containing dimethylaniline monooxygenase 1 (FMO1) is upregulated in the *in vitro* nonalcoholic fatty liver disease (NAFLD) model. (A–C) This study examined lipid accumulation and metabolic indicators in the NAFLD model induced by free fatty acids (FFAs). (D,E) The expression levels of FMO1 mRNA and protein were significantly higher compared to the Control group, indicated by $^{***}p < 0.001$. TG, Triglyceride.

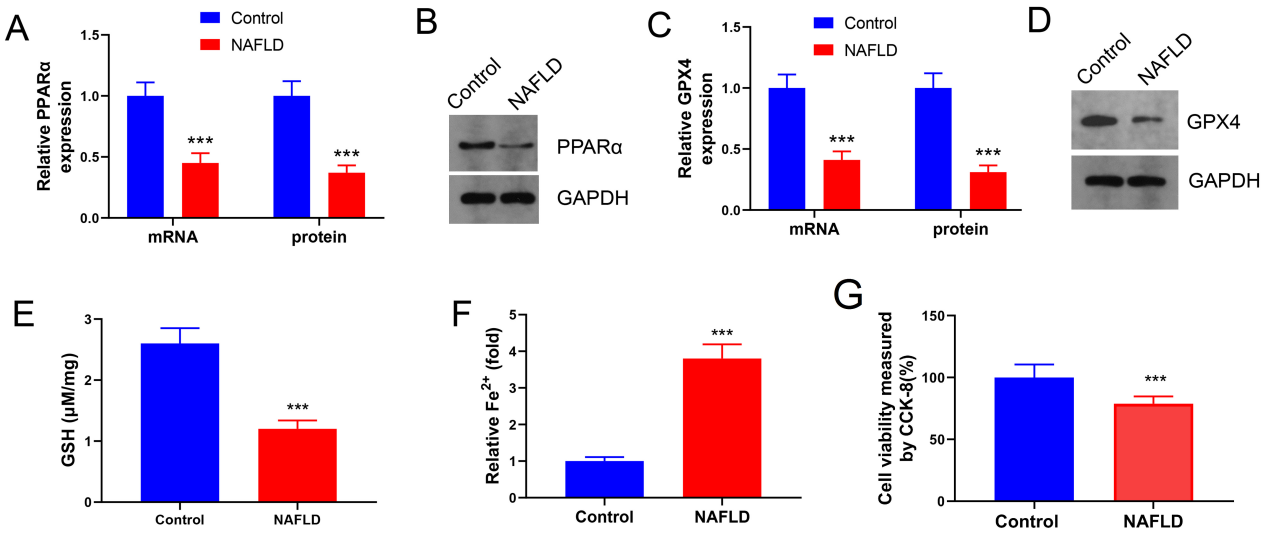

Fig. 2. Peroxisome proliferator activated receptor alpha (PPARα) is downregulated and ferroptosis is upregulated in the *in vitro* NAFLD model. (A,B) The expression levels of PPARα mRNA and protein. (C,D) The levels of glutathione peroxidase 4 (GPX4) mRNA and protein. (E,F) The impact of free fatty acid (FFA) on the hepatocyte levels of glutathione (GSH) and Fe^{2+}. (G) Cell viability measured by cell counting kit-8 (CCK-8) method. $^{***}p < 0.001$ compared to the Control group.

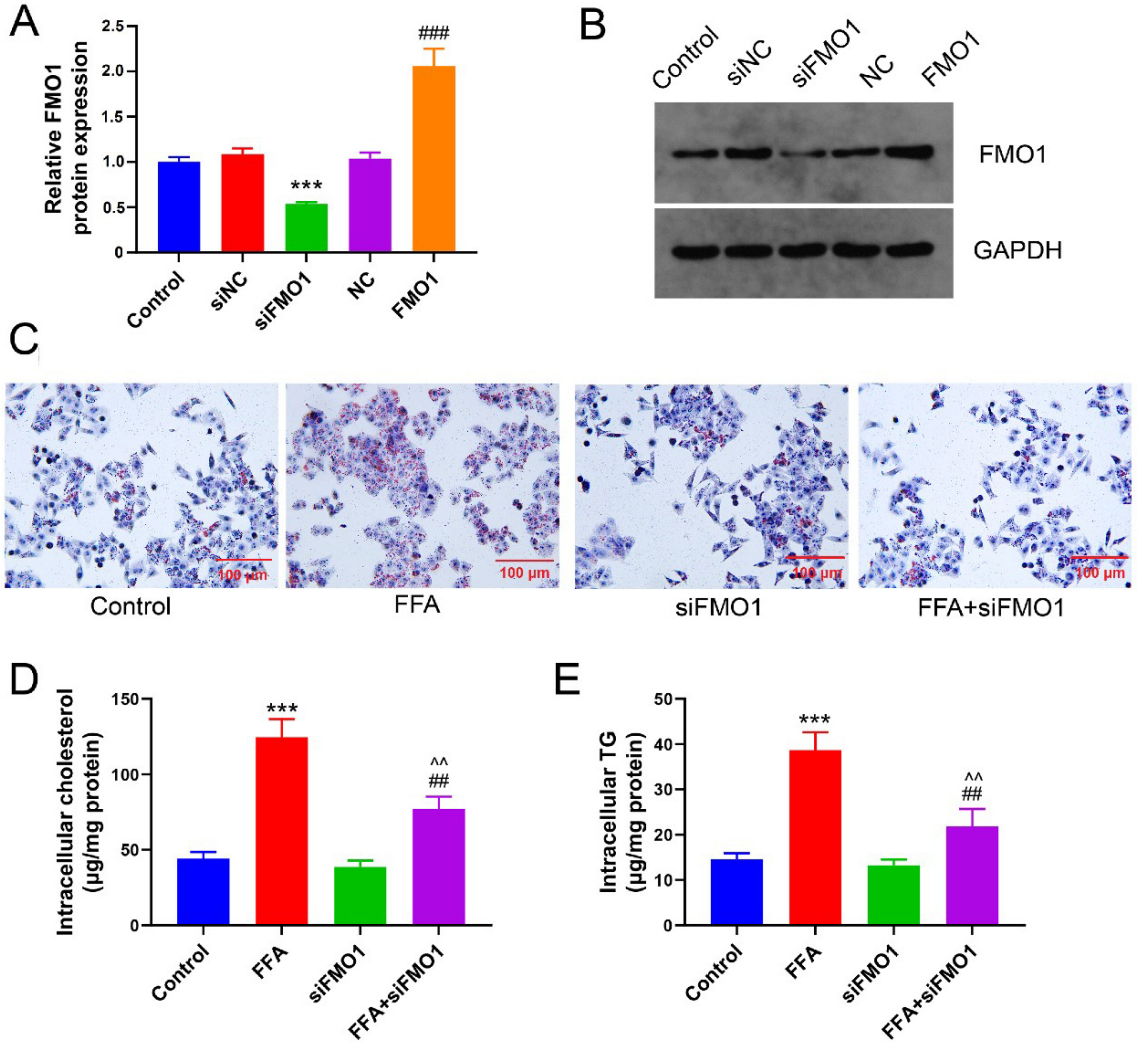

Fig. 3. *FMO1* knockdown suppresses lipid accumulation in the *in vitro* NAFLD model. (A,B) Hepatocytes with *FMO1* knockdown and *FMO1* overexpression were established. (C) The impact of free fatty acids (FFAs) and/or *FMO1* knockdown on lipid accumulation in L02 cells. (D,E) The effects of FFAs and/or *FMO1* knockdown on indicators of lipid metabolism. $^{***}p < 0.001$ compared to Control; $^{\#\#}p < 0.01$, $^{\#\#\#}p < 0.001$ compared to the FFA group; $^{\wedge\wedge}p < 0.01$ compared to the short-interfering RNA against FMO1 (si-FMO1) group. NC, negative control.

a pipette. Subsequently, cells were seeded in fluorescent Petri dishes and incubated with the probe solution in a cell incubator. The cells were then observed under a laser microscope with excitation and emission wavelengths of 532 and 572 nm, respectively. The concentration of Fe^{2+} was calculated relative to the control group.

Statistical Analysis

The data is presented as the mean ± the standard deviation. To compare the means, a one-way analysis of variance was conducted with Tukey's multiple comparison tests (GraphPad Prism version 7.0, GraphPad Software Inc., San Diego, CA, USA). Differences were regarded as significant when the p-value < 0.05.

Results

FMO1 is Upregulated in FFA-Treated L02 Cells

The FFA-treated L02 cells exhibited lipid accumulation and upregulated TG and cholesterol levels, indicating the successful establishment of the NAFLD model (Fig. 1A–C). The levels of FMO1 in FFA-stimulated cells were significantly higher than those in Control cells (Fig. 1D,E, $p < 0.001$).

PPARα is Downregulated and Ferroptosis is Upregulated in the in Vitro NAFLD Model

In the NAFLD model, it was observed that the levels of PPARα were decreased (Fig. 2A,B, $p < 0.001$). The levels of GPX4 were also downregulated following treatment with FFA (Fig. 2C,D, $p < 0.001$). Moreover, FFA caused

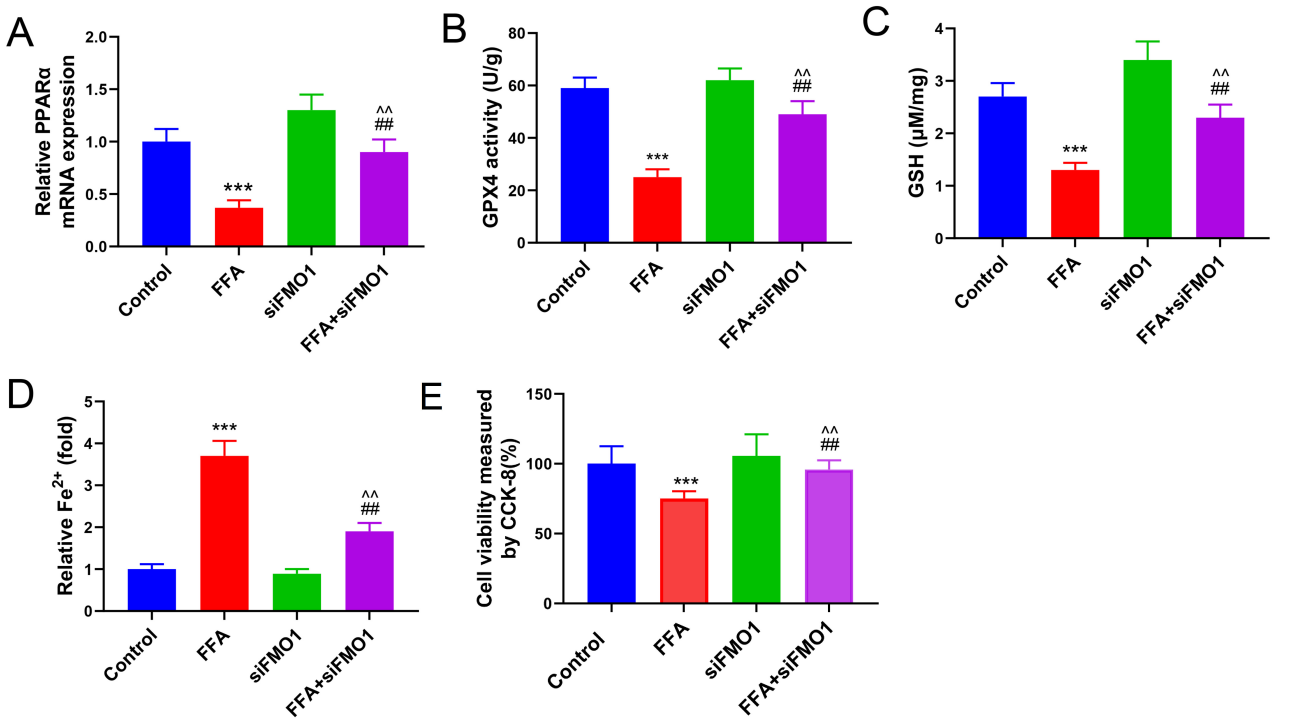

Fig. 4. Knocking down *FMO1* reduces the decrease in peroxisome proliferator activated receptor alpha *(PPARα)* and the increase in ferroptosis in an *in vitro* model of NAFLD. (A) The mRNA levels of *PPARα* are affected by free fatty acids (FFAs) and/or *FMO1* knockdown. (B–D) Ferroptosis is influenced by FFAs and/or *FMO1* knockdown. (E) Cell viability measured by CCK-8 method. $^{***}p < 0.001$ compared to Control; $^{\#\#}p < 0.01$ compared to the FFA group; $^{\wedge\wedge}p < 0.01$ compared to the si-FMO1 group.

a decrease in the GSH level (Fig. 2E, $p < 0.001$) and a significant increase in the intracellular Fe^{2+} level (Fig. 2F, $p < 0.001$). Additionally, the viability of cells was reduced by FFA treatment (Fig. 2G, $p < 0.001$). These findings indicate the occurrence of hepatocyte ferroptosis in NAFLD.

FMO1 Knockdown Suppresses Lipid Accumulation in NAFLD

The researchers conducted rescue experiments to examine the regulatory effects of FMO1 on hepatocyte lipid accumulation, PPARα expression, and ferroptosis in NAFLD. Both *FMO1* knockdown and *FMO1* overexpressing L02 cells were created (Fig. 3A,B, $p < 0.001$). *FMO1* knockdown had a minor inhibitory effect on lipid accumulation and significantly reduced FFA-induced NAFLD (Fig. 3C). The si-FMO1 group showed lower TG and cholesterol levels compared to the Control group. Moreover, the FFA + si-FMO1 group had lower TG and cholesterol levels than the FFA group (Fig. 3D,E, $p < 0.01$). These findings indicate that suppressing *FMO1* through knockdown can inhibit FFA-induced lipid accumulation.

FMO1 Knockdown Mitigates FFA-Induced PPARα Downregulation and Ferroptosis Upregulation in L02 Cells

Afterwards, the researchers investigated the impact of FFA and *FMO1* knockdown on PPARα and ferroptosis. The results showed that *FMO1* knockdown effectively lessened the decrease in *PPARα* mRNA levels induced by FFA (Fig. 4A, $p < 0.01$). In comparison to the Control group, the FFA group exhibited reduced levels of GPX4 and GSH, while levels of Fe^{2+} were increased (Fig. 4B–D, $p < 0.001$). In the FFA + si-FMO1 group, GPX4 and GSH levels were higher than in the FFA group but lower than in the si-FMO1 group (Fig. 4B–D, $p < 0.01$). Moreover, Fe^{2+} levels in the FFA + si-FMO1 group were lower than in the FFA group but higher than in the si-FMO1 group (Fig. 4B–D, $p < 0.01$). The cell viability rate in the FFA + si-FMO1 group was significantly higher than in the FFA group (Fig. 4E, $p < 0.01$). These results indicate that *FMO1* knockdown reduces lipid accumulation and alleviates the downregulation of PPARα and upregulation of ferroptosis induced by FFA. Consequently, these findings shed light on the underlying mechanism of FMO1, providing valuable insights.

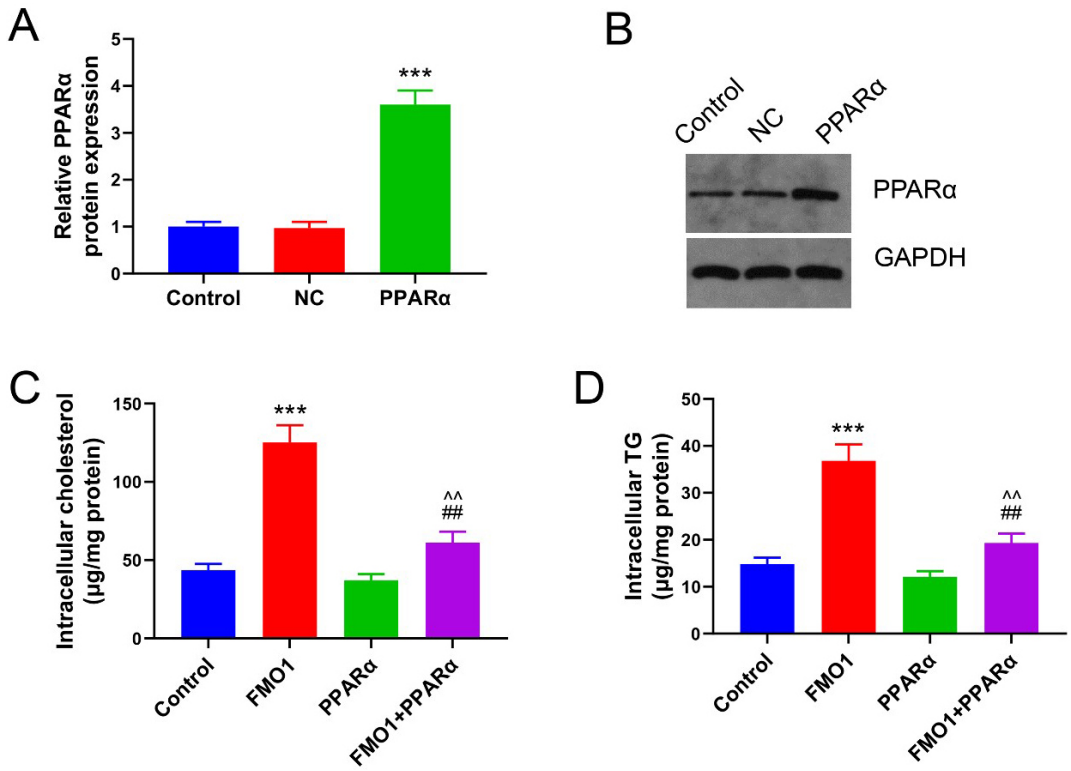

Fig. 5. *PPARα* overexpression suppresses FMO1-induced lipid accumulation. (A,B) Hepatocytes were engineered to have increased levels of PPARα. (C,D) The effect of increasing FMO1 and/or PPARα levels on lipid accumulation was investigated. $^{***}p < 0.001$ compared to Control; $^{\#\#}p < 0.01$ compared to the FMO1 group; $^{\wedge\wedge}p < 0.01$ compared to the PPARα group.

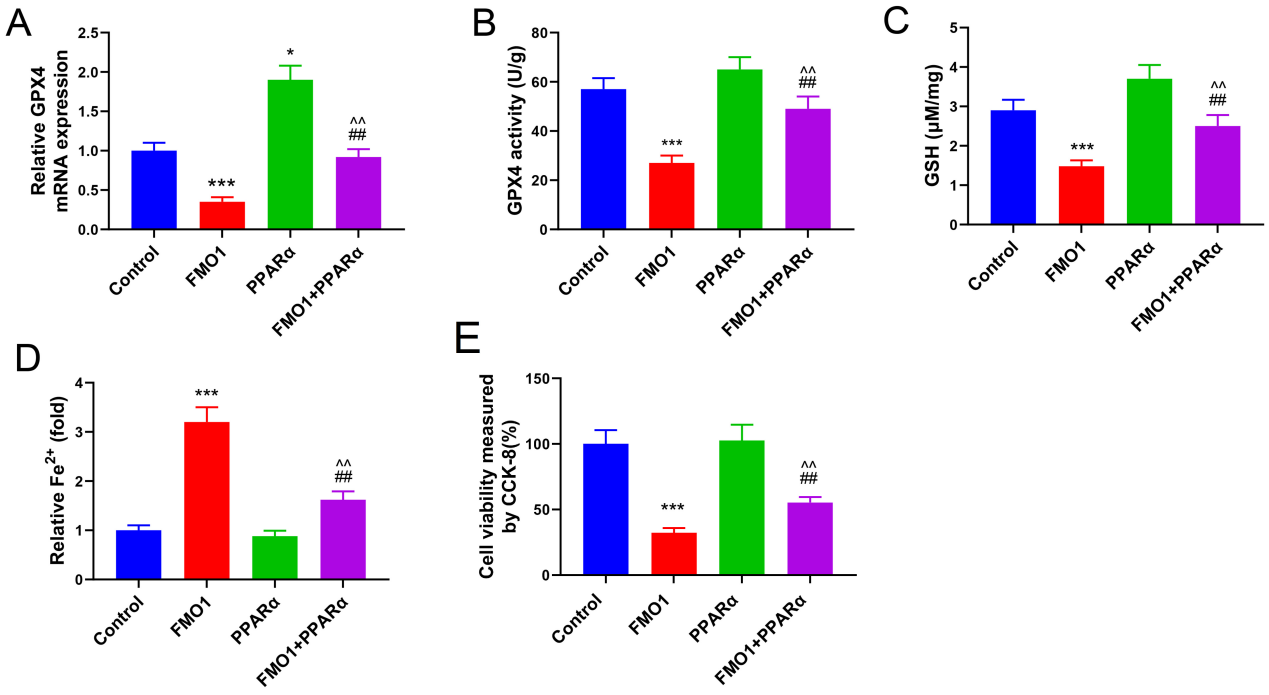

Fig. 6. *PPARα* overexpression suppresses FMO1-induced ferroptosis. (A) Effects of *FMO1* overexpression and/or *PPARα* overexpression on glutathione peroxidase 4 (*GPX4*) transcription. (B–D) Effects of *FMO1* overexpression and/or *PPARα* overexpression on ferroptosis. (E) Cell viability measured by CCK-8 method. $^{*}p < 0.05$ compared to the Control group; $^{***}p < 0.001$ compared with the Control group; $^{\#\#}p < 0.01$ compared with the FMO1 group; $^{\wedge\wedge}p < 0.01$ compared with the PPARα group.

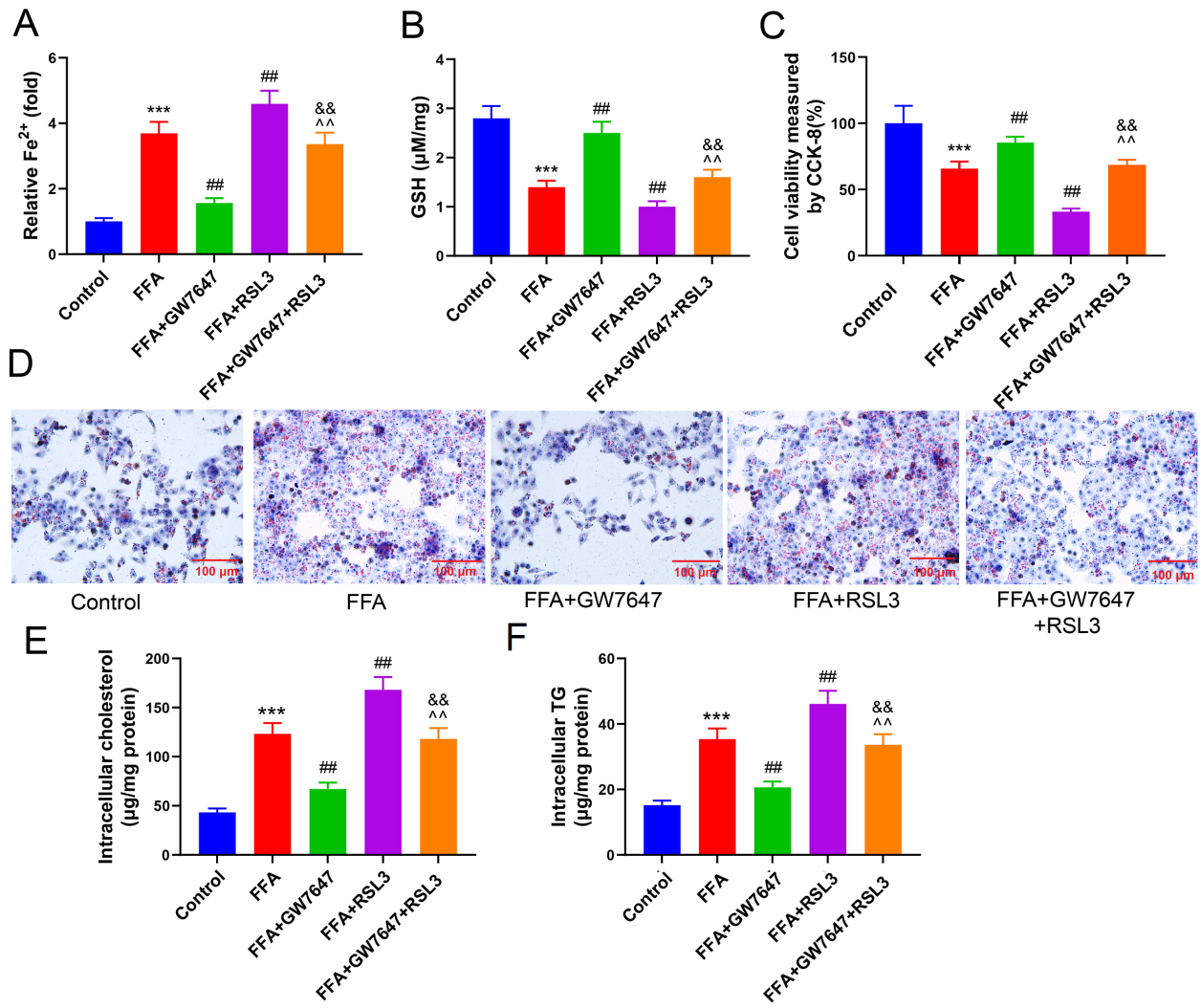

Fig. 7. The alleviating effects of PPARα on lipid accumulation are suppressed when ferroptosis induction occurs in the *in vitro* NAFLD model. (A,B) The levels of Fe^{2+} and glutathione (GSH) in hepatocytes induced by free fatty acids (FFAs) are affected by GW7647 (PPARα agonist) and/or RSL3 (ferroptosis activator). (C) GW7647 and/or RSL3 impact fat accumulation induced by FFA. (D,E) GW7647 and/or RSL3 influence the indicators of lipid metabolism induced by FFA. (F) Intracellular TG levels. $^{***}p < 0.001$ compared with the Control group; $^{\#\#}p < 0.01$ compared with the FFA group; $^{\wedge\wedge}p < 0.01$ compared with the FFA + GW7647 group; $^{\&\&}p < 0.01$ compared with the FFA + RSL3 group.

PPARα Overexpression Inhibits the FMO1-Induced Upregulation of Lipid Accumulation and Ferroptosis in Hepatocytes

The subsequent step involved conducting rescue experiments to explore how FMO1 triggers lipid accumulation and ferroptosis via PPARα. In order to analyze the impact of *FMO1* overexpression and/or *PPARα* overexpression on hepatocytes (Fig. 5A,B), the cells were categorized into four distinct groups: Control, FMO1, PPARα, and FMO1 + PPARα groups. The levels of TG and cholesterol were found to increase in the FMO1 group (Fig. 5C,D, $p < 0.001$) but decrease in the PPARα group (Fig. 5C,D, $p < 0.01$). Additionally, the TG and cholesterol levels in the FMO1 + PPARα group were considerably lower than those in the FMO1 group, but significantly higher than those in the PPARα group (Fig. 5C,D). These observations suggest that FMO1 facilitates lipid accumulation in hepatocytes by means of PPARα.

Furthermore, we investigated the effects of *FMO1* overexpression and/or *PPARα* overexpression on ferroptosis in hepatocytes. Compared to Control, the levels of *GPX4* transcription and activity were significantly reduced in the FMO1 group but increased in the PPARα group. In the FMO1 + PPARα group, the levels of GPX4 were higher than those in the FMO1 group (Fig. 6A,B, $p < 0.01$) but lower than those in the PPARα group (Fig. 6A,B, $p < 0.01$). Additionally, the GSH levels were higher in the FMO1 + PPARα group compared to the FMO1 group (Fig. 6C, $p <$

0.01) but lower than those in the PPARα group (Fig. 6C, $p < 0.01$). The Fe^{2+} levels in the FMO1 + PPARα group were lower than those in the FMO1 group but higher than those in the PPARα group (Fig. 6D, $p < 0.01$). Furthermore, the cell viability was decreased in the FMO1 group ($p < 0.01$; Fig. 6E). However, the cell viability in the FMO1 + PPARα group was higher than that in the Control group ($p < 0.01$; Fig. 6E).

Ferroptosis Induction in the in Vitro NAFLD Model Mitigates the Alleviating Effects of PPARα Overexpression on Lipid Accumulation

To further clarify the effects of PPARα and ferroptosis on NAFLD downstream of FMO1, pharmacological agents were used to induce PPARα activation and/or ferroptosis in the FFA-induced NAFLD model. Comparison between the FFA group and the FFA + GW7647 group showed a downregulation of Fe^{2+} levels and an upregulation of GSH levels (Fig. 7A,B, $p < 0.01$). Moreover, compared to the FFA group, the FFA + RSL3 group exhibited an upregulation of Fe^{2+} levels and a downregulation of GSH levels (Fig. 7A,B, $p < 0.01$). The Fe^{2+} levels in the FFA + GW7647 + RSL3 group were higher than in the FFA + GW7647 group but lower than in the FFA + RSL3 group. The GSH levels in the FFA + GW7647 + RSL3 group were lower than in the FFA + GW7647 group but higher than in the FFA + RSL3 group (Fig. 7A,B, $p < 0.01$).

Furthermore, the FFA + GW7647 group exhibited a significantly higher cell viability rate compared to the FFA group ($p < 0.01$; Fig. 7C), suggesting that PPARα plays a role in regulating ferroptosis in NAFLD. Similarly, the cell viability rate in the FFA + RSL3 group was found to be higher than that in the FFA group ($p < 0.01$; Fig. 7C). The administration of RSL3 worsened abnormal lipid metabolism and hindered the beneficial effects of *PPARα* overexpression on alleviating NAFLD (Fig. 7D–F, $p < 0.01$). Meanwhile, treatment with GW7647 mitigated FFA-induced lipid accumulation and upregulation of TG, cholesterol, and ferroptosis (Fig. 7D–F, $p < 0.01$). These findings suggest that FMO1 alleviates fat accumulation in NAFLD through PPARα by suppressing ferroptosis.

Discussion

NAFLD is characterized by the excessive buildup of lipids in liver cells [23,24]. Among patients diagnosed with NAFLD, 10%–20% of cases rapidly progress to nonalcoholic steatohepatitis [25]. These patients have a 25% risk of developing liver cirrhosis within 10 years and a high risk of cancer, which is a major health threat to patients [26,27]. Therefore, the mechanisms of NAFLD must be elucidated to identify therapeutic targets.

The expression of PPARα, a nuclear receptor, is age-dependent and regulated by brown adipose tissue differentiation, stress, insulin, and leptin and was involved in NAFLD [28,29]. PPARα promotes the entry of fatty acids into the mitochondria for metabolism by inducing the transcription of carnitine palmitoyltransferase 1 (CPT1) [30]. High intake of lipids inhibits the expression of PPARα, leading to lipid accumulation [31]. Therefore, PPARα activation is a potential therapeutic strategy for NAFLD, which has been examined in clinical trials [32,33]. However, the mechanisms underlying the regulatory effects of PPARα on hepatocyte lipid accumulation have not been fully elucidated. Additionally, the mechanisms that regulate the expression of PPARα are unclear. FMO1, an oxygenase, catalyzes the N-oxidation of secondary and tertiary amines and is involved in oxidative metabolism [34].

Sequencing analysis found that FMO1 levels are upregulated in NAFLD tissue [18]. FMO1 is reported to regulate energy homeostasis by modulating fat metabolism [35,36]. This initial study observed an increase in the expression of FMO1 in an *in vitro* NAFLD model. Rescue experiments were conducted to assess the impact of *FMO1* knockdown on NAFLD induced by FFA *in vitro*. The results showed that *FMO1* knockdown successfully reduced the lipid accumulation in hepatocytes caused by FFA. Additionally, *FMO1* knockdown upregulated the expression level of PPARα and effectively mitigated the FFA-induced downregulation of PPARα. Conversely, *FMO1* overexpression promoted aberrant lipid metabolism, which was alleviated upon *PPARα* overexpression. This suggests that FMO1 promotes NAFLD through PPARα. Consistently, previous studies have suggested that FMO1 regulates PPARα. For example, FMO1 promotes renal development and function by regulating PPARα [37]. Additionally, FMO1 mediates the hepatic metabolism of some drugs through PPARα [19]. FMO2 and FMO5, which are related to the FMO1 family, regulate glucose or lipid metabolism in hepatocytes by upregulating PPARα expression [38,39]. The findings of this study and previous studies suggest that FMO1 promotes fat accumulation in NAFLD by inhibiting PPARα. To further analyze the mechanism through which FMO1 promotes NAFLD via PPARα, this study investigated the regulatory effects of FMO1 on ferroptosis.

Recent studies have indicated that iron overload and associated oxidative stress are the primary causes of NAFLD [40–42]. However, the mechanisms underlying the regulation of ferroptosis in NAFLD and its correlation with fat accumulation are unclear. The ferroptosis levels were significantly upregulated in the *in vitro* NAFLD model examined in this study. Furthermore, *FMO1* knockdown upregulated PPARα expression and mitigated the FFA-induced upregulation of ferroptosis. *PPARα* overexpression suppressed the *FMO1* overexpression-induced hepatocyte ferroptosis. Additionally, the induction of ferroptosis in NAFLD inhibited the alleviating effects of PPARα on fat accumulation. Xing *et al.* [16] reported that PPARα alleviates ferroptosis and maintains the liver metabolism balance by directly promoting GPX4 expression. Furthermore,

the inhibition of ferroptosis is reported to prevent some degenerative diseases [15]. Gong *et al*. [43] demonstrated that the homeostasis of PPARα-related ferroptosis mediates disease progression in aldosterone-producing adenomas. These findings suggest that FMO1/PPARα regulates lipid metabolism by modulating ferroptosis.

This study has some limitations. The correlation between FMO1, PPARα, and ferroptosis in NAFLD was not confirmed in clinical samples and animal models. Additionally, the molecular mechanism through which FMO1 promotes PPARα expression and regulates ferroptosis was not elucidated.

Conclusions

FMO1 plays a crucial role in the development of NAFLD by regulating PPARα and ferroptosis. In particular, FMO1 promotes ferroptosis by inhibiting PPARα expression and consequently dysregulates lipid metabolism. Thus, FMO1, PPARα, and ferroptosis are potential therapeutic targets for NAFLD. FMO1 and ferroptosis must be considered when PPARα is targeted for the clinical treatment of NAFLD.

Abbreviations

FMO1, flavin containing dimethylaniline monooxygenase 1; NAFLD, nonalcoholic fatty liver disease; PPARα, peroxisome proliferator activated receptor alpha; FFAs, free fatty acids; GPX4, glutathione peroxidase 4; DMSO, dimethyl sulfoxide; CCK-8, cell counting kit-8; qRT-PCR, Quantitative real-time polymerase chain reaction; ELISA, Enzyme-linked immunosorbent assay; GSH, glutathione.

Availability of Data and Materials

All data and scripts used for analyses are available from the corresponding author.

Author Contributions

LZ, HZ and JM designed the study. LZ, QS, and YL performed the research. ZY analyzed the data. LP did the literature research. JL prepared the figures and participated in the analysis and interpretation of data. All authors contributed to editorial changes in the manuscript. All authors read and approved the final manuscript. All authors have participated sufficiently in the work and agreed to be accountable for all aspects of the work.

Ethics Approval and Consent to Participate

Not applicable.

Acknowledgment

Not applicable.

Funding

This study was supported by the Academic Leaders Training Program of Pudong Health Bureau of Shanghai: No. PWRd2019-12); the Research Grant for Health Science and Technology of Pudong Health Bureau of Shanghai: No. PW2022A-07); the Youth Fund Project of Pudong New Area Gongli Hospital: No. 2020YQNJJ-10).

Conflict of Interest

The authors declare no conflict of interest.

References

[1] Powell EE, Wong VWS, Rinella M. Non-alcoholic fatty liver disease. Lancet. 2021; 397: 2212–2224.

[2] Campos-Murguía A, Ruiz-Margáin A, González-Regueiro JA, Macías-Rodríguez RU. Clinical assessment and management of liver fibrosis in non-alcoholic fatty liver disease. World Journal of Gastroenterology. 2020; 26: 5919–5943.

[3] Kanwal F, Kramer JR, Mapakshi S, Natarajan Y, Chayanupatkul M, Richardson PA, *et al*. Risk of Hepatocellular Cancer in Patients With Non-Alcoholic Fatty Liver Disease. Gastroenterology. 2018; 155: 1828–1837.e2.

[4] Allen AM, Therneau TM, Larson JJ, Coward A, Somers VK, Kamath PS. Nonalcoholic fatty liver disease incidence and impact on metabolic burden and death: A 20 year-community study. Hepatology. 2018; 67: 1726–1736.

[5] Ye Q, Zou B, Yeo YH, Li J, Huang DQ, Wu Y, *et al*. Global prevalence, incidence, and outcomes of non-obese or lean non-alcoholic fatty liver disease: a systematic review and meta-analysis. The Lancet. Gastroenterology & Hepatology. 2020; 5: 739–752.

[6] Cotter TG, Rinella M. Nonalcoholic Fatty Liver Disease 2020: The State of the Disease. Gastroenterology. 2020; 158: 1851–1864.

[7] Sun Y, Chen P, Zhai B, Zhang M, Xiang Y, Fang J, *et al*. The emerging role of ferroptosis in inflammation. Biomedicine & Pharmacotherapy. 2020; 127: 110108.

[8] Zhang Y, Swanda RV, Nie L, Liu X, Wang C, Lee H, *et al*. mTORC1 couples cyst(e)ine availability with GPX4 protein synthesis and ferroptosis regulation. Nature Communications. 2021; 12: 1589.

[9] Sun L, Dong H, Zhang W, Wang N, Ni N, Bai X, *et al*. Lipid Peroxidation, GSH Depletion, and *SLC7A11* Inhibition Are Common Causes of EMT and Ferroptosis in A549 Cells, but Different in Specific Mechanisms. DNA and Cell Biology. 2021; 40: 172–183.

[10] Mancardi D, Mezzanotte M, Arrigo E, Barinotti A, Roetto A. Iron Overload, Oxidative Stress, and Ferroptosis in the Failing Heart and Liver. Antioxidants. 2021; 10: 1864.

[11] Jia M, Zhang H, Qin Q, Hou Y, Zhang X, Chen D, *et al*. Ferroptosis as a new therapeutic opportunity for nonviral liver disease. European Journal of Pharmacology. 2021; 908: 174319.

[12] Zhang H, Zhang E, Hu H. Role of Ferroptosis in Non-Alcoholic Fatty Liver Disease and Its Implications for Therapeutic Strategies. Biomedicines. 2021; 9: 1660.

[13] Pawlak M, Lefebvre P, Staels B. Molecular mechanism of PPARα action and its impact on lipid metabolism, inflammation and fibrosis in non-alcoholic fatty liver disease. Journal of Hepatology. 2015; 62: 720–733.

[14] Kumar DP, Caffrey R, Marioneaux J, Santhekadur PK, Bhat M, Alonso C, *et al*. The PPAR α/γ Agonist Saroglitazar Improves Insulin Resistance and Steatohepatitis in a Diet Induced Animal Model of Nonalcoholic Fatty Liver Disease. Scientific Reports. 2020; 10: 9330.

[15] Venkatesh D, O'Brien NA, Zandkarimi F, Tong DR, Stokes ME, Dunn DE, *et al*. MDM2 and MDMX promote ferroptosis by PPARα-mediated lipid remodeling. Genes & Development. 2020; 34: 526–543.

[16] Xing G, Meng L, Cao S, Liu S, Wu J, Li Q, *et al*. PPARα alleviates iron overload-induced ferroptosis in mouse liver. EMBO Reports. 2022; 23: e52280.

[17] Jia X, Zhai T. Integrated Analysis of Multiple Microarray Studies to Identify Novel Gene Signatures in Non-alcoholic Fatty Liver Disease. Frontiers in Endocrinology. 2019; 10: 599.

[18] Shi C, Pei M, Wang Y, Chen Q, Cao P, Zhang L, *et al*. Changes of flavin-containing monooxygenases and trimethylamine-N-oxide may be involved in the promotion of non-alcoholic fatty liver disease by intestinal microbiota metabolite trimethylamine. Biochemical and Biophysical Research Communications. 2022; 594: 1–7.

[19] Fujino C, Tamura Y, Tange S, Nakajima H, Sanoh S, Watanabe Y, *et al*. Metabolism of methiocarb and carbaryl by rat and human livers and plasma, and effect on their PXR, CAR and PPARα activities. The Journal of Toxicological Sciences. 2016; 41: 677–691.

[20] Li M, Xu C, Shi J, Ding J, Wan X, Chen D, *et al*. Fatty acids promote fatty liver disease via the dysregulation of 3-mercaptopyruvate sulfurtransferase/hydrogen sulfide pathway. Gut. 2018; 67: 2169–2180.

[21] Lee HY, Gao X, Barrasa MI, Li H, Elmes RR, Peters LL, *et al*. PPAR-α and glucocorticoid receptor synergize to promote erythroid progenitor self-renewal. Nature. 2015; 522: 474–477.

[22] Zhu G, Murshed A, Li H, Ma J, Zhen N, Ding M, *et al*. O-GlcNAcylation enhances sensitivity to RSL3-induced ferroptosis via the YAP/TFRC pathway in liver cancer. Cell Death Discovery. 2021; 7: 83.

[23] Raza S, Rajak S, Upadhyay A, Tewari A, Anthony Sinha R. Current treatment paradigms and emerging therapies for NAFLD/NASH. Frontiers in Bioscience (Landmark Edition). 2021; 26: 206–237.

[24] Fan JG, Kim SU, Wong VWS. New trends on obesity and NAFLD in Asia. Journal of Hepatology. 2017; 67: 862–873.

[25] Zhang C, Yang M. Current Options and Future Directions for NAFLD and NASH Treatment. International Journal of Molecular Sciences. 2021; 22: 7571.

[26] Ioannou GN. Epidemiology and risk-stratification of NAFLD-associated HCC. Journal of Hepatology. 2021; 75: 1476–1484.

[27] Anstee QM, Reeves HL, Kotsiliti E, Govaere O, Heikenwalder M. From NASH to HCC: current concepts and future challenges. Nature Reviews. Gastroenterology & Hepatology. 2019; 16: 411–428.

[28] Smati S, Polizzi A, Fougerat A, Ellero-Simatos S, Blum Y, Lippi Y, *et al*. Integrative study of diet-induced mouse models of NAFLD identifies PPARα as a sexually dimorphic drug target. Gut. 2022; 71: 807–821.

[29] Preidis GA, Kim KH, Moore DD. Nutrient-sensing nuclear receptors PPARα and FXR control liver energy balance. The Journal of Clinical Investigation. 2017; 127: 1193–1201.

[30] Moody L, Xu GB, Chen H, Pan YX. Epigenetic regulation of carnitine palmitoyltransferase 1 (Cpt1a) by high fat diet. Biochimica et Biophysica Acta. Gene Regulatory Mechanisms. 2019; 1862: 141–152.

[31] Kim K, Kang JK, Jung YH, Lee SB, Rametta R, Dongiovanni P, *et al*. Adipocyte PHLPP2 inhibition prevents obesity-induced fatty liver. Nature Communications. 2021; 12: 1822.

[32] Gawrieh S, Noureddin M, Loo N, Mohseni R, Awasty V, Cusi K, *et al*. Saroglitazar, a PPAR-α/γ Agonist, for Treatment of NAFLD: A Randomized Controlled Double-Blind Phase 2 Trial. Hepatology. 2021; 74: 1809–1824.

[33] Tutunchi H, Ostadrahimi A, Saghafi-Asl M, Hosseinzadeh-Attar MJ, Shakeri A, Asghari-Jafarabadi M, *et al*. Oleoylethanolamide supplementation in obese patients newly diagnosed with non-alcoholic fatty liver disease: Effects on metabolic parameters, anthropometric indices, and expression of PPAR-α, UCP1, and UCP2 genes. Pharmacological Research. 2020; 156: 104770.

[34] Bailleul G, Nicoll CR, Mascotti ML, Mattevi A, Fraaije MW. Ancestral reconstruction of mammalian FMO1 enables structural determination, revealing unique features that explain its catalytic properties. The Journal of Biological Chemistry. 2021; 296: 100221.

[35] Yeung CK, Lang DH, Thummel KE, Rettie AE. Immunoquantitation of FMO1 in human liver, kidney, and intestine. Drug Metabolism and Disposition: the Biological Fate of Chemicals. 2000; 28: 1107–1111.

[36] Veeravalli S, Omar BA, Houseman L, Hancock M, Gonzalez Malagon SG, Scott F, *et al*. The phenotype of a flavin-containing monooyxgenase knockout mouse implicates the drug-metabolizing enzyme FMO1 as a novel regulator of energy balance. Biochemical Pharmacology. 2014; 90: 88–95.

[37] Martovetsky G, Tee JB, Nigam SK. Hepatocyte nuclear factors 4α and 1α regulate kidney developmental expression of drug-metabolizing enzymes and drug transporters. Molecular Pharmacology. 2013; 84: 808–823.

[38] Shih DM, Wang Z, Lee R, Meng Y, Che N, Charugundla S, *et al*. Flavin containing monooxygenase 3 exerts broad effects on glucose and lipid metabolism and atherosclerosis. Journal of Lipid Research. 2015; 56: 22–37.

[39] Kong L, Chen J, Ji X, Qin Q, Yang H, Liu D, *et al*. Alcoholic fatty liver disease inhibited the co-expression of Fmo5 and PPARα to activate the NF-κB signaling pathway, thereby reducing liver injury via inducing gut microbiota disturbance. Journal of Experimental & Clinical Cancer Research. 2021; 40: 18.

[40] Fernandez M, Lokan J, Leung C, Grigg A. A critical evaluation of the role of iron overload in fatty liver disease. Journal of Gastroenterology and Hepatology. 2022; 37: 1873–1883.

[41] Ucar F, Sezer S, Erdogan S, Akyol S, Armutcu F, Akyol O. The relationship between oxidative stress and nonalcoholic fatty liver disease: Its effects on the development of nonalcoholic steatohepatitis. Redox Report: Communications in Free Radical Research. 2013; 18: 127–133.

[42] Videla LA, Valenzuela R. Perspectives in liver redox imbalance: Toxicological and pharmacological aspects underlying iron overloading, nonalcoholic fatty liver disease, and thyroid hormone action. BioFactors. 2022; 48: 400–415.

[43] Gong S, Tetti M, Reincke M, Williams TA. Primary Aldosteronism: Metabolic Reprogramming and the Pathogenesis of Aldosterone-Producing Adenomas. Cancers. 2021; 13: 3716.